Egypt. J. Chem. **Vol. 67,** No. 4 pp. 273 - 278 (2024)

Egyptian Journal of Chemistry

http://ejchem.journals.ekb.eg/

Impact of the Purification Procedure on the Properties of All-inorganic CsPbI3-xBrx Mixed-halide Perovskite Quantum Dots

Maha Hussein[1], Ahmed A. Farghali[2], Fabienne Barroso-Bujans[3,4,5], and Laila Saad[*1, 3,4]

[1] Renewable Energy Science and Engineering Department, Faculty of Postgraduate Studies for Advanced Sciences (PSAS), Beni-Suef University, Beni Suef, 62511, Egypt.
[2] Materials Science and Nanotechnology Department, Faculty of Postgraduate Studies for Advanced Sciences (PSAS), Beni-Suef University, Beni Suef, 62511, Egypt.
[3] Donostia International Physics Center (DIPC), Paseo Manuel Lardizábal 4, 20018 Donostia−San Sebastian, Spain
[4] Materials Physics Center, CSIC-UPV/EHU, Paseo Manuel Lardizábal 5, 20018 Donostia−San Sebastian, Spain
[5]KERBASQUE - Basque Foundation for Science, María Díaz de Haro 3, E-48013 Bilbao, Spain

Abstract

The field of photovoltaic research is witnessing significant growth in the study of organic-inorganic perovskites, primarily due to their promising optoelectronic properties and the notable increase in their power conversion efficiency (PCE). Despite the advantageous characteristics exhibited by lead halide-based perovskites, such as their suitability as absorbers, the issue of instability remains a prominent concern. To address this challenge, we propose a potential solution involving the partial doping of all-inorganic perovskite $CsPbI_3$ quantum dots (PQDs) with bromine. This approach not only aims to mitigate the instability problem but also allows for the customization of the band gap of pure cesium lead bromide $CsPbBr_3$. Furthermore, we explore the impact of solvent selection and the choice of precipitating agent on the stability of the resulting quantum dots. Through the implementation of a hot injection method, we successfully synthesized perovskite quantum dots (PQDs) and conducted an analysis of their optical, structural, and thermal properties. X-ray diffraction analysis revealed the cubic phase of the prepared mixed halide $CsPbI_{3-x}Br_x$ PQDs.

Keywords: All-inorganic Perovskite, QD solar cells, Cesium lead halides

1. Introduction

Organometallic perovskite is the most emerging topic of research among recent photovoltaic generation technologies since it showed a high power conversion efficiency (PCE).[1] ABX3 perovskite crystal structure acts as an active layer for light-harvesting.[2] PSCs can be easily fabricated by the wet chemical process and are less expensive than the traditional silicon solar cell. Researches are attempting to improve the efficiencies of PSCs to the Shockley–Queisser limit[3]. While, the major obstacles are low surface area of the photoanode and high recombination of the interfacial charge carrier. Other problem is the instability and poor life time which are serious threats for the commercialization of PSCs [4]. Substitution of the unstable organic group with more durable inorganic Cs^+ cations form all-inorganic perovskites as cesium lead halide system ($CsPbX_3$, X is halide) yields in stable perovskites which are more stable temperature and humidity factors [4]. However, the instability of these materials against moisture and heat is a great obstacle for their long-term applications. Despite growing interest, understanding on the fundamental properties the inorganic $CsPbX_3$ is still insufficient. Some studies have addressed this concern, and another potential approach involves substituting some of the Pb^{2+} with different metallic elements.[5] Further studies on inorganic perovskite optical and electronic properties can provide important insights into overcoming problems like energy losses and stability toxicity [6].

*Corresponding author e-mail: laila.saad.h@gmail.com.; (L. Saad).
Receive Date: 14 January 2024, Revise Date: 21 January 2024, Accept Date: 14 February 2024
DOI: https://doi.org/10.21608/ejchem.2024.262811.9186

In this work $CsPbBr_3$ and $CsPbI3\text{-}xBr_x$ are synthesized via hot injection technique; throughout the purification procedure of colloidal nanocrystals (PQDs), there were apprehensions arising from the observed discoloration and phase transformation, which raised concerns about potential degradation. The PQDs solution, originally displaying vivid green ($CsPbBr_3$) and pink ($CsPbI_{3-x}Br_x$) hues, underwent a change, becoming pale yellow or white at two distinct stages of the purification process: after the introduction of the precipitation agent and following centrifugation. In order to tackle this issue, we conducted an investigation into the influence of the type and quantity of the anti-solvent and washing agents, as well as different centrifugation times, on the efficacy of the purification process.

2. Materials and Methods

Synthesis of Perovskite Quantum Dots

The hot-injection method for Quantum Dots (QDs) involves conducting reactions at temperatures typically ranging from 90 to 240 °C. This method employs a rapid injection process to effectively separate the nucleation and growth stages, leading to more uniform colloidal nanocrystal QD dispersions. The success of this method relies on the nucleation and growth processes being slower than the effective mixing times of the precursor solution. However, achieving this for QDs has been challenging due to experimental evidence showing that nucleation occurs within a very short time frame of 0.4 seconds. Recent theoretical studies have also suggested that nucleation processes themselves take place on even faster time scales, measured in sub-microseconds [7]. This rapid kinetics has hindered detailed experimental investigations into the early formation stages of perovskites in QDs synthesis. Despite these challenges, the typical hot injection synthesis of QDs follows equations 1 and 2, representing the generalized conversion of precursors into their reactive species, with the overall formation reaction described by equation 3. Despite the availability of these reaction mechanisms, the specific details of the underlying nucleation mechanism remain uncertain.

$$Cs_2CO_3 + 2OA \longrightarrow 2CsOA + H_2O + CO_2 \quad (1)$$

$$PbX + 2OA + 2OLA \longrightarrow PbOA_2 + 2OLAX \quad (2)$$

$$CsOA + PbOA_2 + 3OLAX \longrightarrow CsPbX_3 + 3OA^- + 3OLA^+ \quad (3)$$

Initially, the cesium precursor was prepared as Cs-oleate, 0.814 g of cesium carbonate, 2.5 ml of oleic acid and 40 ml of octadecene were mixed and magnetically stirred and dried under vacuum and heated under N_2 gas for 60 min at 150°C. The mixture was purged with nitrogen for 10 min, and back under vacuum. This process repeated three times, until the solution was turned clear. The prepared Cs-oleate solution was stored under N_2 at 70°C before use. [8, 9] And for the PQDs preparation a mixture containing 10 ml of octadecene, 0.138 g of lead bromide (for $CSPbBr_3$), and a combination of 0.104 g of lead iodide and 0.055 g of lead bromide (for cesium lead bromide iodide mixed halide quantum dots) was prepared. The mixture was placed in a three-neck flask and subjected to heating at 120°C for one hour under vacuum while stirring [10]. Meanwhile, a blend of 0.6 ml of oleic acid and 0.6 ml of oleylamine was heated under nitrogen at 70°C and then added to the flask. The solution was maintained under vacuum at 120°C for 30 minutes until the lead iodide completely dissolved, resulting in a clear solution. Subsequently, the temperature was further raised to 160°C for 10 minutes under vacuum. Following this, 0.8 mL of the prepared Cs-Oleate was preheated and swiftly injected into the mixture. Controlling the quantity of Cs-oleate is crucial as an excessive amount leads to the gradual transformation of cubic CsPbBr3 nanocrystals into rhombohedral Cs4PbBr6 crystals.[11] After a 5-second interval, the flask was immediately immersed in an ice bath to halt the reaction. The solution color changed to bright green and bright pink for $CsPbBr_3$ and $CsPbI_{3-x}Br_x$, respectively (if you think it is revelant you can add a picture showing the colors of your samples).

The hot-injection (HI) method operates between 90 to 240°C, swiftly separating nucleation and growth stages for uniform nanocrystal dispersions. Nucleation in PQDs happens rapidly within 0.4 seconds. Formation involves PbX_6 polyhedral as nuclei gradually filled with A+ ions, similar to bulk perovskite. To maintain PQDs size consistency, the reaction should be stopped after 5 seconds in an ice bath, yielding smaller particles at lower temperatures.[7]

Purification of the colloidal PQDs

During the purification process of the colloidal nanocrystals (PQDs), the observed discoloration and phase transformation raised concerns about their degradation. The PQDs solution, initially bright green ($CsPbBr_3$), and pink ($CsPbI_{3-x}Br_x$), turned pale yellow or white during two purification steps: after adding the precipitation agent and after centrifugation. To address this issue, we investigated the impact of precipitation agent type and quantity, as well as centrifugation time, on the purification

process. We found that the type and amount of the precipitation agent and the duration of centrifugation were critical parameters. Toluene and acetone- as anti-solvent agents- were found to instantly damage the crystals and cause solution discoloration, indicating its unsuitability as a precipitation agent. Moreover, an excess amount of MeOAC resulted in PQDs degradation during centrifugation. Among the tested precipitation agents, a 1:1 mixture of hexane and MeOAC (3 mL each) demonstrated the highest stability. To determine the optimal conditions, First 10 mL of MeOAC was used as anti-solvent agent, then we adjusted the co-washing agents to 3 mL of MeOAc and 3 mL of hexane, and the centrifugation time to 6 min at 6000-8000 rpm. These optimized conditions provided the most stable PQDs, ensuring minimal decomposition and maintaining their original properties throughout the purification process [12]

3. Results and discussion

Characterization techniques of synthesized PQDs

Ultraviolet–visible (UV–Vis) spectroscopy

The transmission and absorption spectra of PDQs were obtained in the range of 300–900 nm using a Shimadzu 2040 UV–Vis spectrophotometer following literature method[13].

Photoluminescence (PL)

Photoluminescence is the re-emission of light after absorption of incident photons by semiconductor materials with energy greater than bandgap energy (Eg). The excited carriers in higher energy levels relax to the available level in ground state by emitting a photon. Photoluminescence measurements were recorded for the PQDs films on glass substrate. [14] PL measurements were carried out at room temperature with a Perkin Elmer LS-55 fluorescence spectrophotometer.

Transmission electron microscope (TEM)

Images of transmission electron microscopy (TEM) were obtained using a JEM-2010 F electron microscope from JEOL-Japan with an accelerating voltage of 200 kV.

X-ray difraction (XRD)

The phase and crystallinity were detected and identified using PANalytical X'pert Pro PW3040 MPD X-Ray Diffract meter (XRD) using copper CuK α radiation (λ=0.15406 nm) in the range of 5° to 80° 2θ at a scan rate of $3°s^{-1}$.

Differential scanning calorimetry (DSC)

Differential scanning calorimetry (DSC) measurements of $CsPbI_{3-x}Br_x$ PQDs were carried out on ~4 mg specimens using a Q2000 TA Instruments. The sample was measured in a sealed aluminum pan from 30 to 350 ºC at 10 °C/min heating and cooling ramps repeated twice. A helium flow rate of 25 mL/min was used.

Thermogravimetric analysis (TGA)

Thermogravimetric analysis (TGA) of $CsPbI_{3-x}Br_x$ PQDs was conducted in a TGA Q500 from TA Instruments by using a constant heating rate of 10 °C/min from room temperature to 800 °C and nitrogen flow of 60 mL/min. Reliability of sample temperature was carefully checked from the derivative thermogravimetric (DTG) peak corresponding to the Curie temperature of nickel.

Structure and crystallinity of PQDs

The crystalline structure of synthesized PQDs was examined using the X-ray diffraction (XRD) technique, and the results are illustrated in Figure 1. In Figure 1A, the diffraction patterns of the $CsPbBr_3$ PQDs, which were purified under the suggested optimal purification conditions (a 1:1 mixture of hexane and MeOAC, 3 mL each, at 8000 rpm for 6 min), revealed the formation of α-cubic phase. This phase exhibits distinct sharp characteristic peaks at 2Θ = 14.5 ° and 25 °, corresponding to (100) and (200) crystal planes, respectively. However, in Figure 1B, the diffraction pattern indicates the presence of characteristic peaks related to the undesired transformed δ-orthorhombic phase for the colloidal purification carried out using an excess of MeOAC [15]. On the other hand, Figure 1C shows the diffraction pattern of the mixed halide $CsPbI_{3-x}Br_x$ PQDs, which were purified using a mixed solution, these PQDs exhibit a cubic phase, displaying a high-intensity peak at 2Θ = 23°.[16, 17]

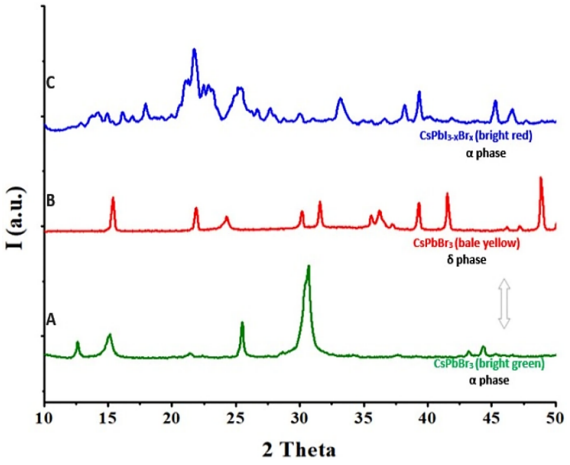

Figure 1: X-ray diffraction patterns of (A) $CsPbBr_3$ PQDs purified with 1:1 hexane and MeOAC mixture, (B) $CsPbBr_3$ PQDs purified with MeOAC, and (C) $CsPbI_{3-x}Br_x$ PQDs purified with 1:1 hexane and MeOAC mixture.

Optical Properties of PQDs

The photoluminescence (PL) and UV-Vis spectroscopy were employed to investigate the optical properties of the PQDs, and the findings are presented in Figures 2 (A and B). The UV−Vis absorption spectrum of the cesium lead bromide PQDs solution demonstrates a robust absorption in the visible-light range, extending up to 570 nm, similar to the behaviors observed for $CsPbI_{3-x}Br_x$.[18] Moreover, the band gap of cesium bromide halides QDs can be adjusted by varying the fractional content of halide.[19] By utilizing the Tuac equation[19], the optical band gap of the prepared PQDs was computed, resulting in estimated values of 2.4 eV for $CsPbBr_3$ and 2.1 eV for $CsPbI_{3-x}Br_x$, respectively.

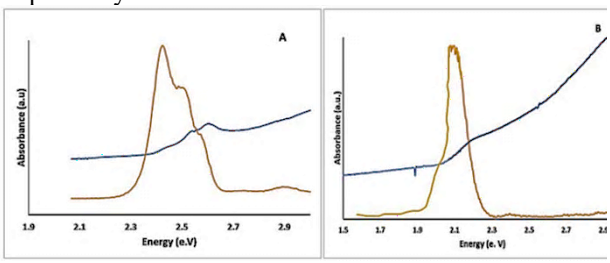

Figure 2: UV-Vis absorbance spectra with PL spectrum (inset) for(A) $CsPbBr_3$, and (B) $CsPbI_{3-x}Br_x$ PQDs.

Morphological properties of PQDs films

Alongside the observed change in color of $CsPbBr_3$ PQDs from bright green to pale yellow, the transmission electron microscopy (TEM) images exhibit the presence of a metastable intermediate phase γ, which eventually progresses to the undesirable final phase δ, as depicted in Figure 3. Additionally, the X-ray diffraction (XRD) patterns highlight the phase transformation and confirm the presence of the yellow phase δ.[6] However, Figures 4 and 5 show the cubic phases for $CsPbBr_3$ and mixed halide which were purified using the 1:1 MeOAC and hexane mixture, with a lattice distance of 3.5 Angstrom, for the mixed halide QDs.

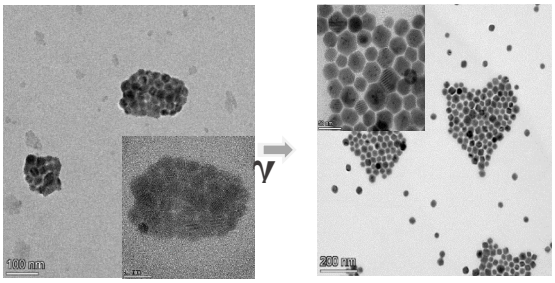

Figure 3: TEM images of the transition metastable intermediate γ and δ phases of $CsPbBr_3$ QDs

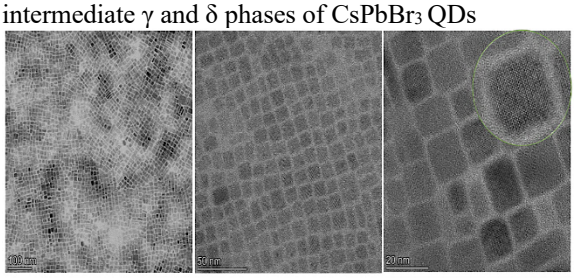

Figure 4: TEM images of the synthesized stable α-cubic phase of $CsPbBr_3$ QDs.

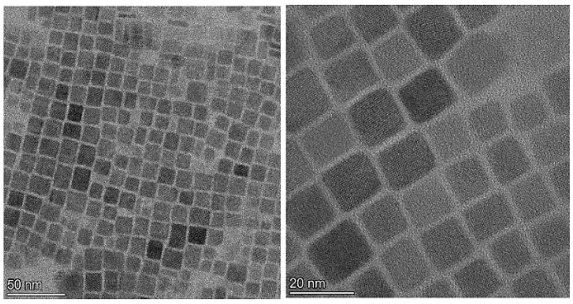

Figure 5: TEM images of the synthesized α-cubic phase $CsPbI_{3-x}Br_x$ QDs.

Thermal behavior of PQDs

The thermal stability of $CsPbI_{3-x}Br_x$ mixed halide QDs was investigated using thermogravimetric analysis (TGA) (Figure 6A). The TGA curve showed an initial weight loss of 4% at 133 ˚C, 2% at 200 ºC and 6 % at 300 ºC attributed to the evaporation of excess solvent. Decomposition starts to occur above 400 ºC as previously observed for $CsPbI_3$ indicating similar thermal stability[6]. The TGA profile showed two steps with maxima of the derivative at 545 and 650 ˚C and 72 % weight loss.

To evaluate the phase transformation of $CsPbI_{3-x}Br_x$ PQDs, the sample was characterized by differential scanning calorimetry (DSC) (Figure 6B). The heating and cooling curves were obtained by first heating the sample from 30 to 350 °C at 10 ºC/min where residual solvent was evaporated. Then, the sample was cooled back to 30 ºC and heated to 350 ºC at a same heating rate. The data of Figure 6B represents the DSC thermogram of the second heating and cooling ramps. The data exhibited an endothermic peak under heating likely indicating a phase transformation occurring at 332 °C. By measuring the area under the endothermic peak and considering that the sample had 10 % of solvent (TGA data), the enthalpy of this process was

determined to be 3.1 J/g. Subsequently, the material exhibited an exothermic process at 280 °C which can be attributed to the reformation of previous phase. In prior studies, the emphasis lay in phase transformation. A metastable γ-$CsPbI_3$ perovskite phase was successfully achieved by manipulating the tilt of [PbI6]4− octahedra through pressure, typically between 0.1 and 0.6 GPa. This involved subjecting yellow δ-$CsPbI_3$ to pressure, heat, and rapid cooling. Interestingly, the emergence of α-$CsPbI_3$ at higher temperatures seemed instrumental in the formation of γ-$CsPbI_3$.[20] PQDs offer alternatives with greater stability compared to the renowned $CH_3NH_3PbI_3$ organic perovskite for solar cell applications. This specific perovskite demonstrates thermal stability only up to 200˚C before it begins to undergo thermal decomposition.[21]

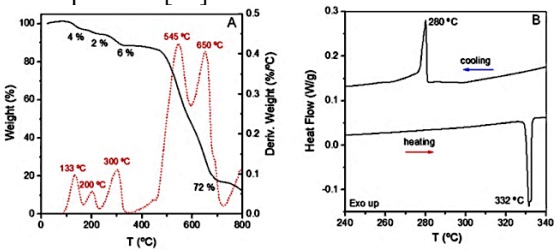

Figure 6: (A) TGA and (B) DSC data of $CsPbI_{3-x}Br_x$ PQDs. (A) The temperature at the maximum of the derivative and weight losses are indicated.

Conclusions

The preparation conditions, particularly the purification step, exert a substantial influence on the ultimate phase of the PQDs. The impact of purification solvents, purification duration, and centrifugation speed on the final characteristic of $CsPbBr_3$ and $CsPbI_{3-x}Br_x$ PQDs were systematically examined and fine-tuned to achieve the desired cubic phase, which is critical for efficient photovoltaic applications.

Acknowledgments

We gratefully acknowledge support from the Donostia International Physics Center (DIPC), San Sebastian, Spain and SCIENCE BY WOMEN program, 5th edition, Women for Africa Foundation, Madrid, Spain. And to the facilities provided by STDF Project (YRG- 33421)

Declarations

Conflicts of interest/Competing interests

No conflict of interest

Availability of data and material

All data generated are included in the paper.

References

[1] Q. Fu and A. K. Y. Jen, "Perovskite solar cell developments, what's next?," *Next Energy,* vol. 1, no. 1, p. 100004, 2023/03/01/ 2023, doi: https://doi.org/10.1016/j.nxener.2023.100004.

[2] X. Zhang *et al.*, "Excellent exciton luminescence of CsPbI3 red quantum dots in borate glass," *Journal of Non-Crystalline Solids,* vol. 541, p. 120066, 2020/08/01/ 2020, doi: https://doi.org/10.1016/j.jnoncrysol.2020.120066.

[3] G. Magdy, M. E. Harb, A. M. Elshaer, L. Saad, S. Ebrahim, and M. Soliman, "Preparation of Electrolytic Quasi-Solid-State Nanofibers for Dye-Sensitized Solar Cells," *JOM,* Article vol. 71, no. 6, pp. 1944-1951, 2019, doi: 10.1007/s11837-019-03404-z.

[4] H. H. AbdElAziz, M. Taha, W. M. A. El Rouby, M. H. Khedr, and L. Saad, "Evaluating the performance of Cs2PtI6−xBrx for photovoltaic and photocatalytic applications using first-principles study and SCAPS-1D simulation," *Heliyon,* Article vol. 8, no. 10, 2022, Art no. e10808, doi: 10.1016/j.heliyon.2022.e10808.

[5] G. C. Adhikari, S. Thapa, H. Zhu, and P. Zhu, "Mg2+-Alloyed All-Inorganic Halide Perovskites for White Light-Emitting Diodes by 3D-Printing Method," *Advanced Optical Materials,* vol. 7, no. 20, 2019, doi: 10.1002/adom.201900916.

[6] S. Dastidar, C. J. Hawley, A. D. Dillon, A. D. Gutierrez-Perez, J. E. Spanier, and A. T. Fafarman, "Quantitative Phase-Change Thermodynamics and Metastability of Perovskite-Phase Cesium Lead Iodide," (in eng), *J Phys Chem Lett,* vol. 8, no. 6, pp. 1278-1282, Mar 16 2017, doi: 10.1021/acs.jpclett.7b00134.

[7] C. K. Ng, C. Wang, and J. J. Jasieniak, "Synthetic Evolution of Colloidal Metal Halide Perovskite Nanocrystals," *Langmuir,* vol. 35, no. 36, pp. 11609-11628, 2019/09/10 2019, doi: 10.1021/acs.langmuir.9b00855.

[8] M. Yue *et al.*, "Optimizing the Performance of CsPbI3-Based Perovskite Solar Cells via Doping a ZnO Electron Transport Layer Coupled with Interface Engineering," *Nano-Micro Letters,* vol. 11, p. 91, 10/18 2019, doi: 10.1007/s40820-019-0320-y.

[9] S. Poncé, M. Schlipf, and F. Giustino, "Origin of Low Carrier Mobilities in Halide Perovskites," *ACS Energy Letters,* vol. 4, no. 2, pp. 456-463, 2019/02/08 2019, doi: 10.1021/acsenergylett.8b02346.

[10] C. Liu *et al.*, "Efficiency and stability enhancement of perovskite solar cells by introducing CsPbI3 quantum dots as an interface engineering layer," *NPG Asia Materials,* vol. 10, no. 6, pp. 552-561, 2018/06/01 2018, doi: 10.1038/s41427-018-0055-0.

[11] G. C. Adhikari, S. Thapa, H. Zhu, A. Grigoriev, and P. Zhu, "Synthesis of CsPbBr3 and Transformation into Cs4PbBr6 Crystals for White Light Emission with High CRI and Tunable CCT," *The Journal of Physical Chemistry C,* vol. 123, no. 18, pp. 12023-12028, 2019, doi: 10.1021/acs.jpcc.9b03369.

[12] K. Wang *et al.*, "All-inorganic cesium lead iodide perovskite solar cells with stabilized efficiency beyond 15," (in eng), *Nat Commun,* vol. 9, no. 1, p. 4544, Oct 31 2018, doi: 10.1038/s41467-018-06915-6.

[13] Y. Chen, J. Yang, S. Wang, Y. Wu, N. Yuan, and W.-H. Zhang, "Interfacial Contact Passivation for Efficient and Stable Cesium-Formamidinium Double-Cation Lead Halide Perovskite Solar Cells," *iScience,* vol. 23, no. 1, p. 100762, 2020/01/24/ 2020, doi: https://doi.org/10.1016/j.isci.2019.100762.

[14] R. Grisorio *et al.*, "Exploring the surface chemistry of cesium lead halide perovskite nanocrystals," *Nanoscale,* 10.1039/C8NR08011A vol. 11, no. 3, pp. 986-999, 2019, doi: 10.1039/C8NR08011A.

[15] A. Soosaimanickam, K. Jeyagopal Ram, and B. Sridharan Moorthy, "Cesium lead halide (CsPbX3, X=Cl, Br, I) perovskite quantum dots-synthesis, properties, and applications: a review of their present status," *Journal of Photonics for Energy,* vol. 6, no. 4, p. 042001, 10/1 2016, doi: 10.1117/1.JPE.6.042001.

[16] L. Yuan, R. Patterson, X. Wen, Z. Zhang, G. Conibeer, and S. Huang, "Investigation of anti-solvent induced optical properties change of cesium lead bromide iodide mixed perovskite (CsPbBr(3-x)I(x)) quantum dots," (in eng), *J Colloid Interface Sci,* vol. 504, pp. 586-592, Oct 15 2017, doi: 10.1016/j.jcis.2017.06.017.

[17] S. Wang, L. Du, Z. Jin, Y. Xin, and H. Mattoussi, "Enhanced Stabilization and Easy Phase Transfer of CsPbBr3 Perovskite Quantum Dots Promoted by High-Affinity Polyzwitterionic Ligands," *Journal of the American Chemical Society,* vol. 142, no. 29, pp. 12669-12680, 2020/07/22 2020, doi: 10.1021/jacs.0c03682.

[18] D. Ghosh, M. Y. Ali, D. K. Chaudhary, and S. Bhattacharyya, "Dependence of halide composition on the stability of highly efficient all-inorganic cesium lead halide perovskite quantum dot solar cells," *Solar Energy Materials and Solar Cells,* vol. 185, pp. 28-35, 2018/10/01/ 2018, doi: https://doi.org/10.1016/j.solmat.2018.05.002.

[19] Y. Zhou, J. Chen, O. M. Bakr, and H.-T. Sun, "Metal-Doped Lead Halide Perovskites: Synthesis, Properties, and Optoelectronic Applications," *Chemistry of Materials,* vol. 30, no. 19, pp. 6589-6613, 2018/10/09 2018, doi: 10.1021/acs.chemmater.8b02989.

[20] F. Ke *et al.*, "Preserving a robust CsPbI(3) perovskite phase via pressure-directed octahedral tilt," *Nat Commun,* vol. 12, no. 1, p. 461, Jan 19 2021, doi: 10.1038/s41467-020-20745-5.

[21] R. K. Singh, S. R. Dash, R. Kumar, N. Jain, and J. Singh, "Role of organic and inorganic cations on thermal behavior of lead iodide perovskites," 2018.